Electronic Supplementary Information

Linkage engineering mediated carriers transfer and surface reaction over carbon nitride for enhanced photocatalytic activity

Shilian Yang,[a,#] Qian Wang,[a,#] Qiuchen Wang,[a] Gen Li,[a] Tianxiang Zhao,[a] Peng Chen,[a,*] Fei Liu[a,*] and Shuang-Feng Yin[b,*]

[a] Provincial Guizhou Key Laboratory of Green Chemical and Clean Energy Technology, School of Chemistry and Chemical Engineering, Guizhou University, Guiyang 550025, Guizhou, China

[b] State Key Laboratory of Chemo/Biosensing and Chemometrics, Provincial Hunan Key Laboratory for Cost-effective Utilization of Fossil Fuel Aimed at Reducing Carbon-dioxide Emissions, College of Chemistry and Chemical Engineering, Hunan University, Changsha 410082, Hunan, China

E-mail: pchen3@gzu.edu.cn (P. Chen), ce.feiliu@gzu.edu.cn (F. Liu) sf_yin@hnu.edu.cn (S. F. Yin)

[#] These authors contribute equally to this work

Table S1. Estimation of O, C and N contents of as-fabricated samples by XPS.

Samples	C	N	O
C_3N_4	46.9	50.8	2.3
COCN-1	16.2	78.7	5.1
COCN-2	44.9	51.5	3.6
COCN-3	38.5	58.9	2.6

Table S2. Binding energy and area ratio of C 1s over as prepared samples

Samples	C–H2		C=C		C–NH		N=C–N		C–O	
	BE (eV)	Area ratio (%)	BE (eV)	Area ratio (%)	BE (eV)	Area ratio (%)	BE (eV)	Area ratio (%)	BE (eV)	Area ratio (%)
C_3N_4	-	-	284.6	26.37	286.3	6.29	288.2	67.34	-	-
COCN-1	284.1	5.4	284.6	18.0	286.0	2.7	287.8	64.5	287.4	9.4
COCN-2	284.1	6.9	284.6	13.2	286.1	1.8	287.8	72.0	287.3	6.1
COCN-3	284.1	3.2	284.6	9.4	286.6	2.3	287.9	79.4	287.7	5.7

Table S3. Binding energy and area ratio of N 1s over as prepared samples

Samples	C-N=C		N-(C3)		$N-H_X$	
	BE (eV)	Area ratio (%)	BE (eV)	Area ratio (%)	BE (eV)	Area ratio (%)

C_3N_4	398.3	76.94	399.7	14.64	400.7	8.42
COCN-1	398.5	73.44	399.7	14.49	400.9	12.07
COCN-2	398.4	74.65	399.7	15.16	400.9	10.19
COCN-3	398.6	75.05	400.1	16.22	401.1	8.73

Table S4. Binding energy and area ratio of O 1s over as prepared samples

Samples	Adsorbed oxygen		Adsorbed H_2O		C-O	
	BE (eV)	Area ratio (%)	BE (eV)	Area ratio (%)	BE (eV)	Area ratio (%)
COCN-1	531.5	62.1	532.6	30.6	533.7	7.3
COCN-2	531.6	62.2	532.7	31.5	533.7	6.3
COCN-3	531.6	63.4	532.7	31.5	533.8	5.1

Table S5. Comparison of different catalysts for photocatalytic HER.

Ref.	Catalysts	Reaction Condition	Time (h)	Oxidant	Conv. (%)	Sel. (%)
S1	Wrinkled C_3N_4 nanosheets	thioanisole (0.5 mmol), methanol (5 mL), $\lambda > 400$ nm, R.T.	1	Air	60	>99
S2	CdS/C_3N_4	thioanisole (0.3 mmol), catalyst (5 mg), methanol (3 mL), $\lambda > 420$ nm, R.T.	6	O_2	61.88	>99
S3	C_{60}/g-C_3N_4	thioanisole (0.2 mmol), catalyst (30 mg), CH3OH (5 mL), $\lambda > 400$ nm, R.T.	10	Air	94.35	100
S4	Nb_2O_5	thioanisole (0.25 mmol), catalyst (25 mg), CH_3OH (0.5 mL), ARS (0.5 mmol), TEMPO (5 mmol), green LEDs, R.T.	1.3	O_2	94	>99

S5	BN@TTCOP	thioanisole (0.2 mmol), catalyst (10 mg), CH_3OH (3.0 mL), LED lamp, R.T.	8	O_2	>99	>99
S6	polydopamine @ TiO_2	thioanisole (0.3 mmol), catalyst (50 mg), TEMPO (0.015 mmol), 460 nm blue LEDs, CH_3OH (1 mL), R.T.	6	O_2	86	81
S7	IEP-7	thioanisole (0.3 mmol), EtOH/H_2O (2 mL), green-LED irradiation (λ=525 nm), R.T.	24	H_2O	77	100
S8	Zr_6−Irphen	thioanisole (0.25 mmol), catalyst (4 mol %), H_2O (4 mL), blue LED, R.T.	12	O_2	100	100
S9	Zr_{12}-NBC	thioanisole (0.3 mmol), catalyst (2 mol % ratio), methanol (4 mL). blue LED, R.T.	10	Air	100	100
S10	C,N-TiO_2	thioanisole (0.3 mmol), acetonitrile (5 mL), 300 W Xe lamp	6	Air	100	100
S11	DhaTph-Zn	catalyst (10 mg), thioanisole (0.05 mmol), CH_3CN (2 mL) and CH_3OH (1 mL), λ > 400 nm.	10	O_2	82	>99
S12	Pt@ imine-based COF	Thioanisole (0.3 mmol) catalyst (2.4 mg), CH3OH (2 mL), blue light.	8	O_2	100	100
S13	anthraquinone functionalized COF linked by β-ketoenamines	thioanisole (0.1 mmol), photocatalyst (10 mg), CH_3CN (2.0 mL), λ = (400−780 nm)	3	O_2	>99	97
S14	C_{60}@PCN-222	photocatalyst (20 mg), thioethers (0.2 mmol), CH_3OH (5 mL), λ > 400 nm	3	Air	>99	100
S15	Incorporated carbonyl	thioanisole (0.5 mmol), photocatalyst (5 mg),	8	O_2	>99	>99

	groups in g-C_3N_4	acetonitrile (2 mL), xenon lamp (50 W) without filter				
This work	COCN-2	thioanisole (0.5 mmol), photocatalyst (20 mg), acetonitrile (2 mL), λ > 420 nm	3	Air	>99	>99

Table S6. Zeta potentials of the as-prepared photocatalysts.

Test time	C_3N_4 (mV)	COCN-3 (mV)	COCN-2 (mV)	COCN-1 (mV)
1	-37.53	-62.28	-71.63	-66.04
2	-42.35	-67.07	-73.29	-68.70
3	-41.04	-68.20	-77.42	-65.52
4	-41.02	-63.24	-75.36	-66.77
5	-42.57	-61.37	-74.94	-64.53
6	-42.32	-60.96	-76.83	-66.63
Average	-41.14	-63.85	-74.91	-66.37

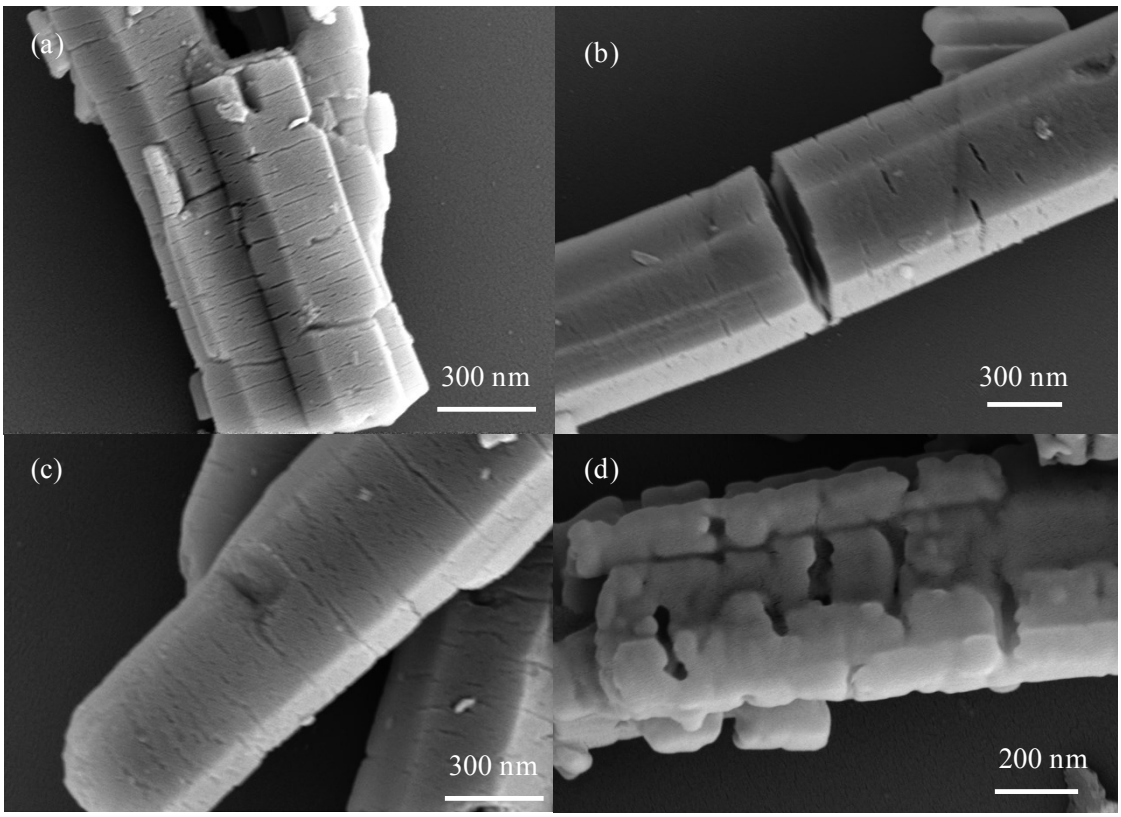

Fig. S1. SEM images of (a) melem, (b) trimethylohmelem, (c) precursor and (d) COCN-2.

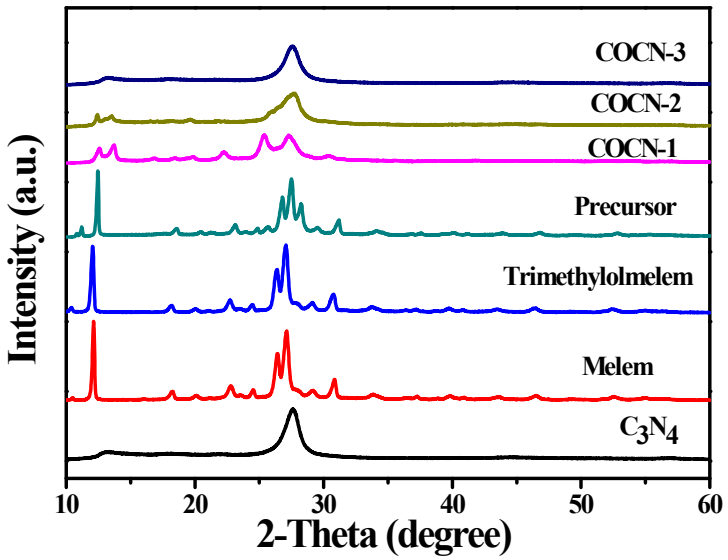

Fig. S2. XRD patterns of as-fabricated samples.

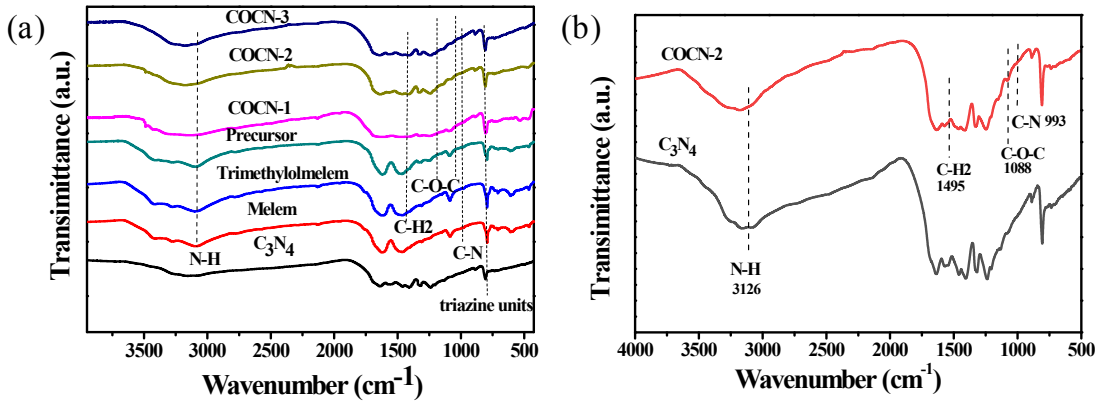

Fig. S3. FTIR spectra of as-fabricated samples.

The structure of COCN was analysed through FTIR spectra to confirm carbon and C-O-C incorporation, as shown in Fig. S3. The signal at 811 cm^{-1} is assigned to the heptazine rings of the conjugated C_3N_4 heterocycles. The broad peaks between 2900 cm^{-1} and 3500 cm^{-1} belong to hydroxyl (−OH) and N−H stretching, indicating that the NH and OH groups exist in the COCN and trimethylolmelem, respectively. The new bands can be observed at 993 cm^{-1} (C−N), 1495 cm^{-1} (C−H2) and 3126 cm^{-1} (N−H), implying the generation of N-CH2-N species in the structure of COCN and precursor.[S16-S18] Furthermore, the characteristic mode of the C–O–C vibration appears at 1088 cm^{-1} in COCN and precursor,[S19-S20] suggesting the synthesis of materials exist two forms chains as illustrated in Fig. 1a.

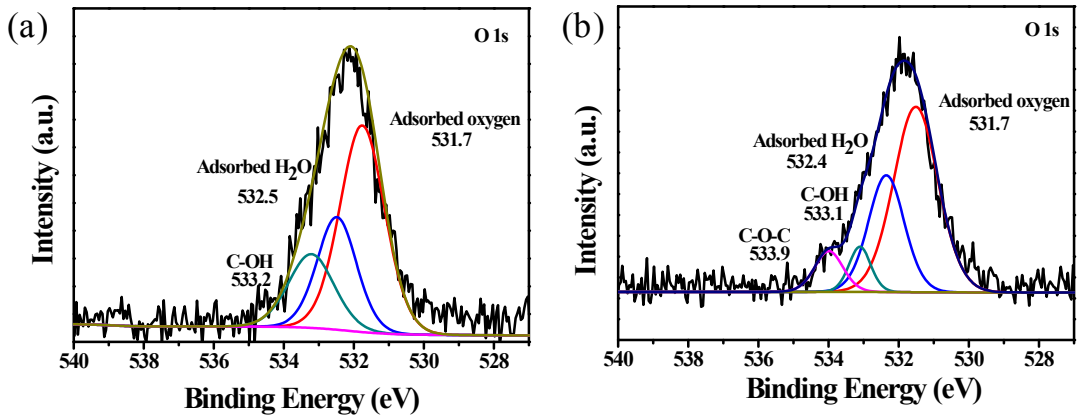

Fig. S4. O1s high-resolution spectra of (a) trimethylohmelem and (b) precursor.

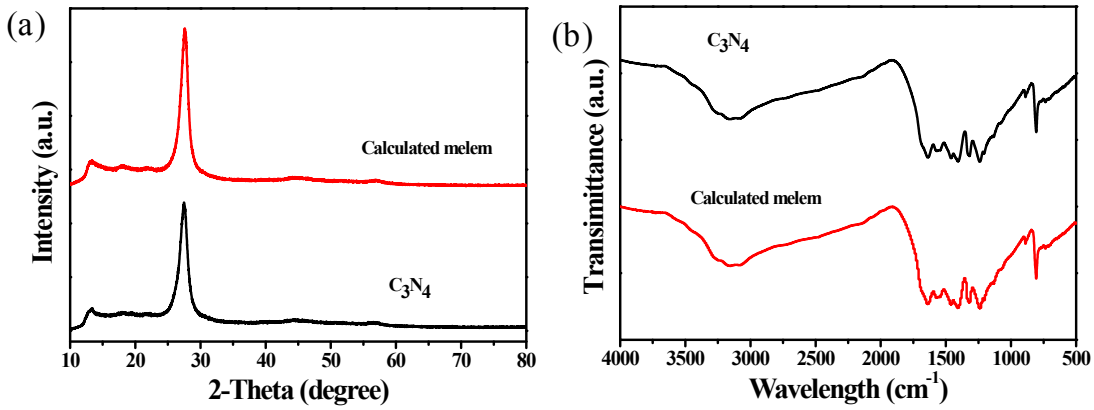

Fig. S5. (a) XRD patterns and (b) FTIR spectra of as-fabricated samples.

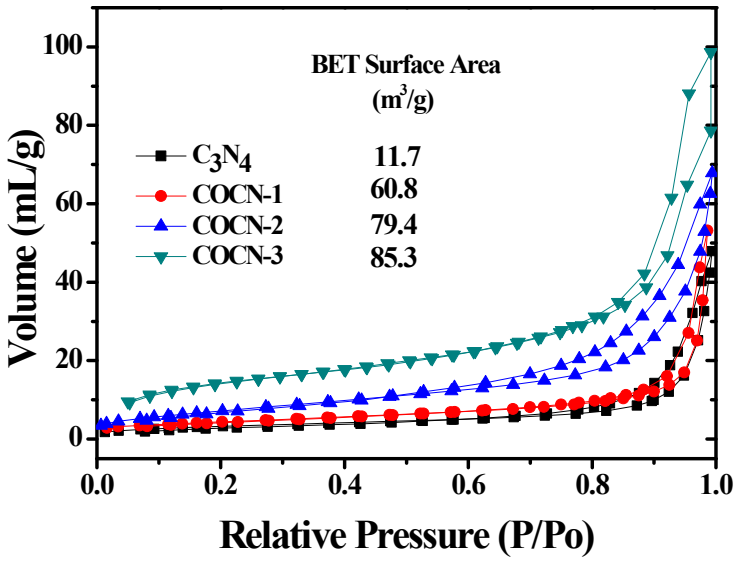

Fig. S6. N_2 sorption isotherms of as-fabricated with the BET surface area data provided as inset.

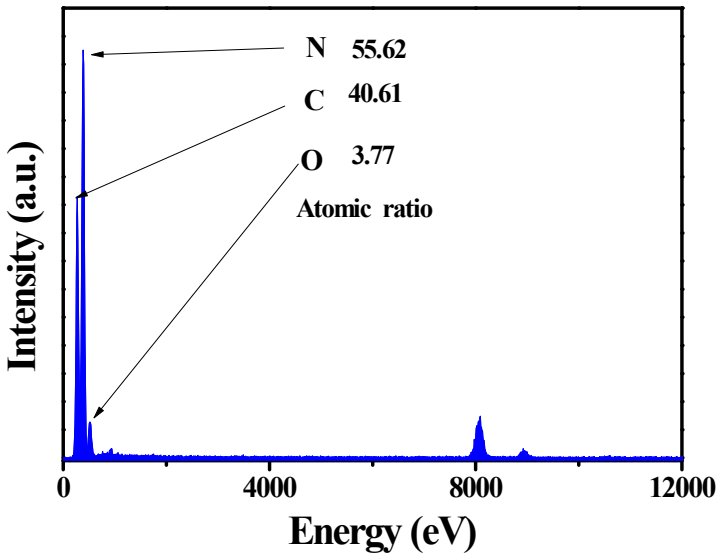

Fig. S7. EDS images of COCN-2.

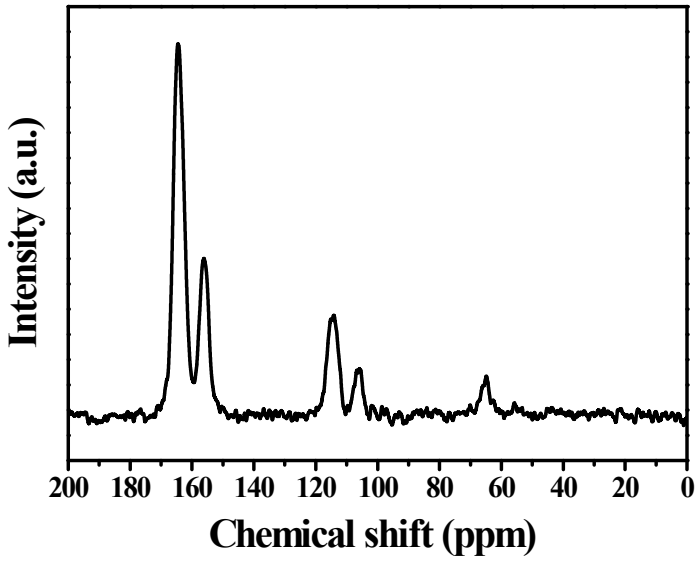

Fig. S8. solid-state 13C NMR spectra of COCN-2.

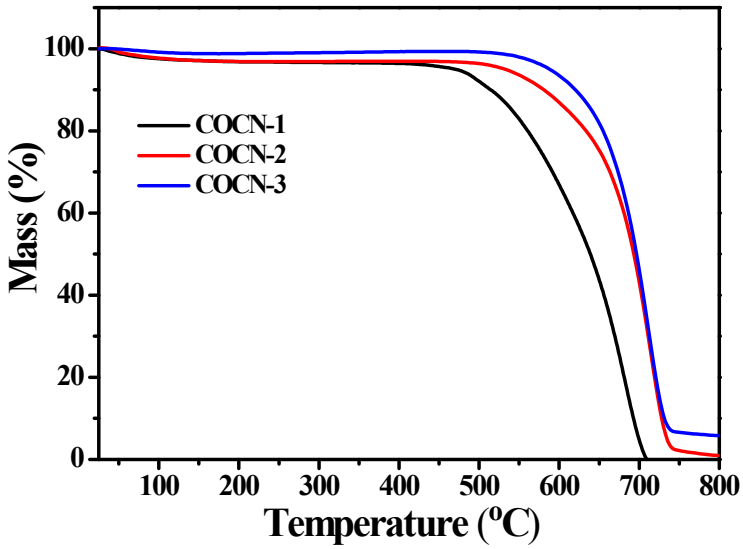

Fig. S9. The TG curves of COCN-1, COCN-2 and COCN-3

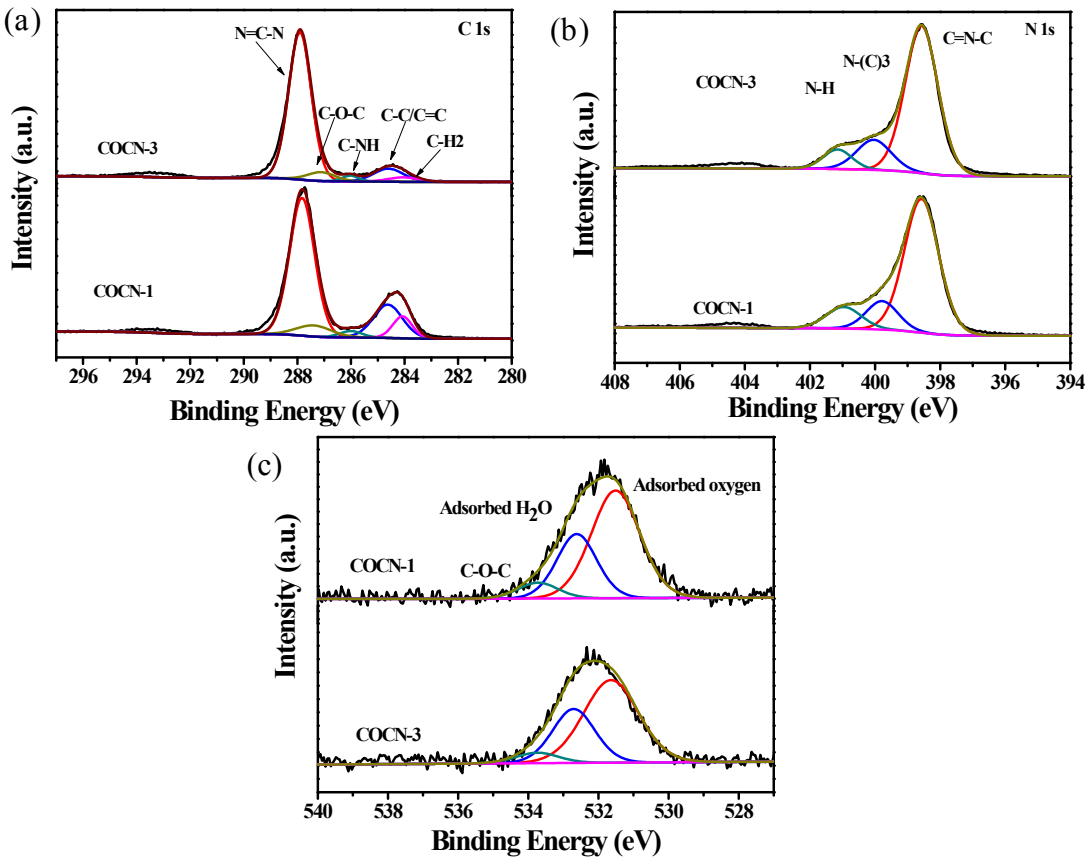

Fig. S10. High-resolution XPS spectra of COCN-1 and COCN-3: (a) C 1s, (b) N 1s and (c) O 1s.

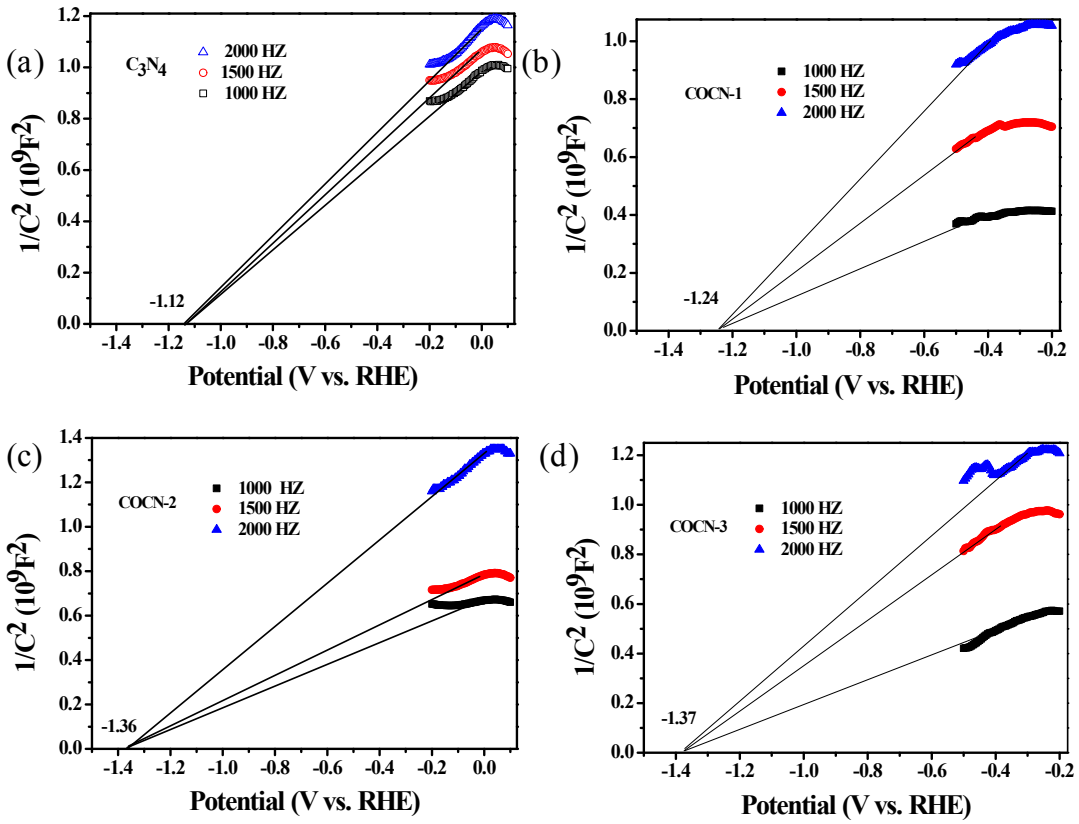

Fig. S11. Mott-Schottky plots of fabricated samples: (a) C_3N_4, (b) COCN-1, (c) COCN-2 and (d) COCN-3.

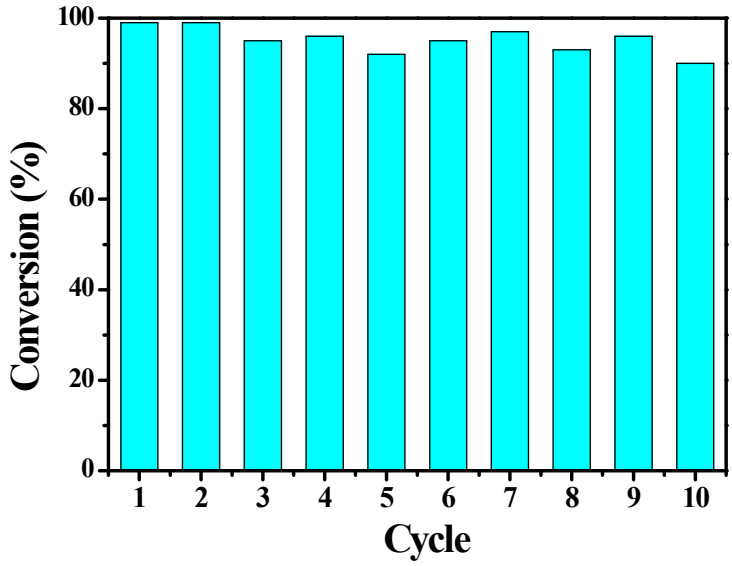

Fig. S12. Cycling test of photocatalytic selective oxidation of sulfides over COCN-2.

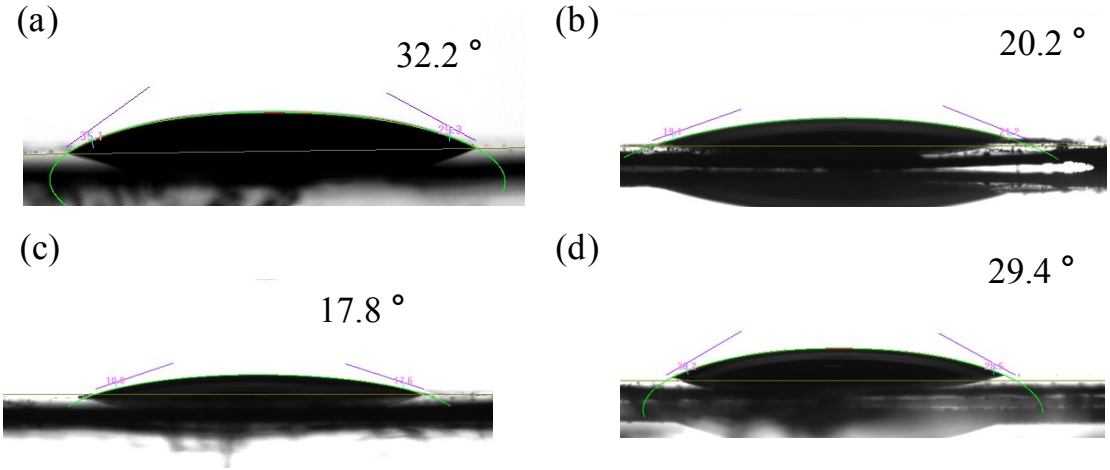

Fig. S13. Contact-angle of thioanisole on the surface of (a) C_3N_4, (b) COCN-1, (c) COCN-2 and (d) COCN-3.

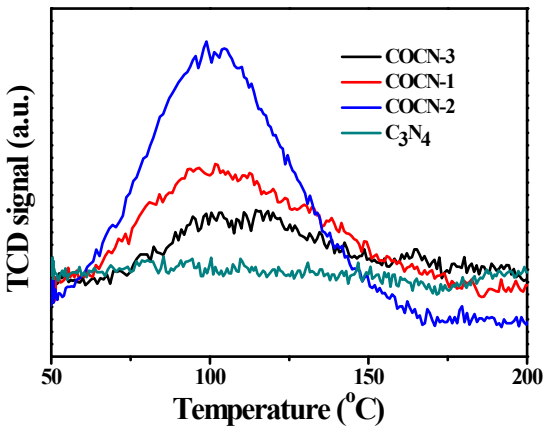

Fig. S14. O_2-temperature programmed desorption spectra of fabricated samples.

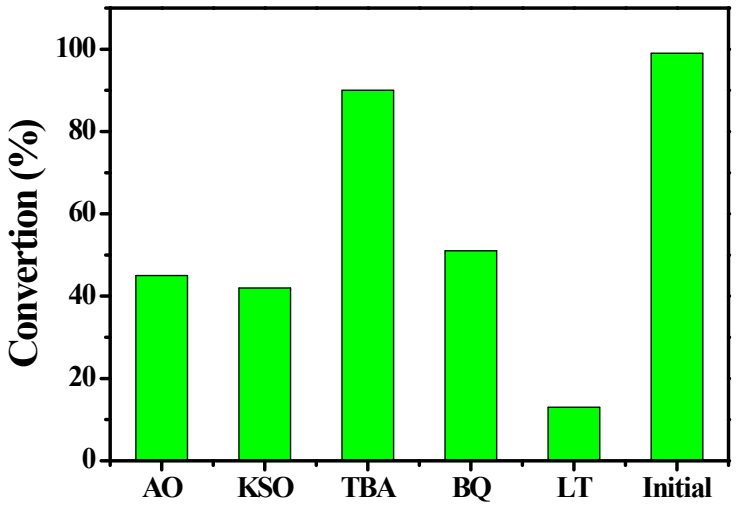

Fig. S15. Photocatalytic selective oxidation of sulfides over COCN-2 with or without a scavenger. Ammonium oxalate (AO), Potassium persulfate (KSO), p-benzoquinone (BQ) and tert-butanol (TBA) as scavengers for hole (h^+), electron (e^-), superoxide radical ($O_2^{\bullet-}$) and hydroxyl radical (·OH) trapping, respectively.

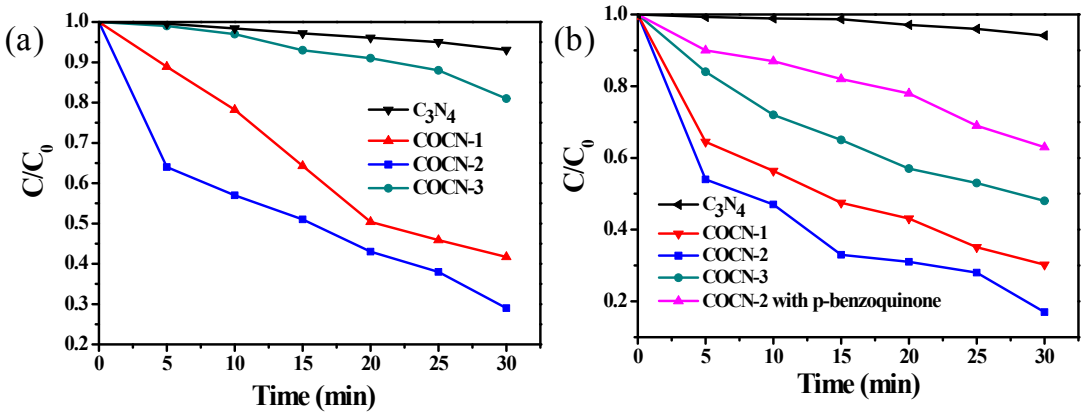

Fig. S16. Photocatalytic degradation of (a) Nitro blue tetrazolium (NBT) and (b) 1,3-diphenylisobenzofuran (DPBF) over different catalysts.

Superoxide radical detection: Briefly, the reaction mixture contained acetonitrile (10 mL), catalyst (20 mg) and nitro blue tetrazolium (NBT, 20 mg). Prior to

irradiation, the mixture was magnetically stirred in the dark for 30 min to establish adsorption-desorption equilibrium. The light source was a 300 W Xe-arc lamp equipped with a 420 nm filter to cut off UV light. The amount of superoxide radicals was identified by a Cary-100 spectrophotometer to record the absorbance change at the wavelength of 280 nm. The mole ratio of generated superoxide radicals and degraded NBT was 4:1 according to the report of Wei et al.[S21]

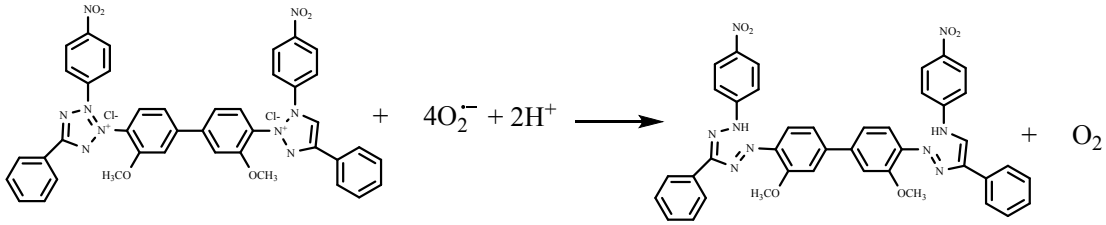

Singlet oxygen detection: Briefly, the reaction mixture contained acetonitrile (10 mL), catalyst (20 mg), and 1,3-diphenylisobenzofuran (DPBF, 20 mg). The light source was a 300 W Xe-arc lamp equipped with a 420 nm filter to cut off UV light. The concentration of singlet oxygen was identified by a Cary-100 spectrophotometer to record the absorbance change at the wavelength of 410 nm. The mole of generated singlet oxygen was calculated by the report of Chen et al.[S22]

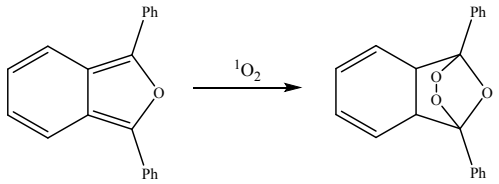

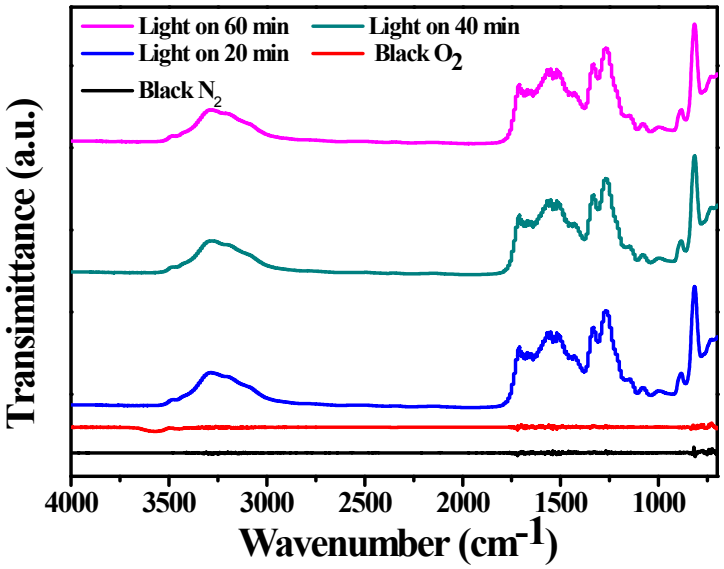

Fig. S17. *In situ* FT-IR spectra of COCN-2.

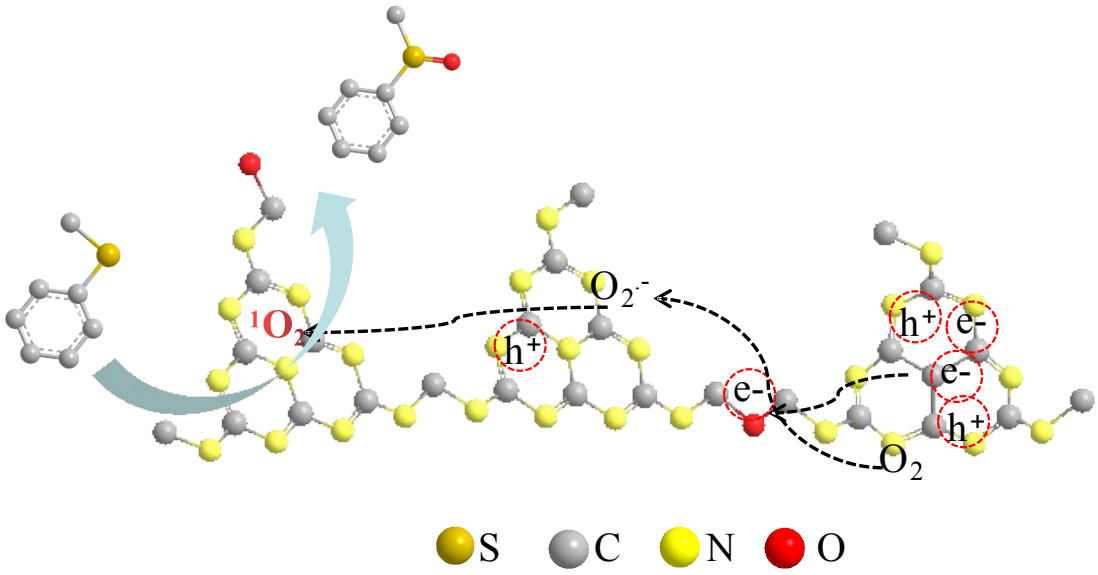

Fig. S18. Plausible mechanism for the photocatalytic selective oxidation of sulfides over COCN-2 under visible light irradiation.

Based on the above results and the relevant mechanisms reported in the literature,[S23-S24] a plausible mechanism for this photocatalytic oxidation over COCN-2 is proposed in Fig. S18. Under light illumination, COCN-2 was easily photoexcited

and produced electrons and holes pairs. Photogenerated electrons will react to the surface of O_2 to form a radical species $O_2^{\bullet-}$. Subsequently, then a quantity of $O_2^{\bullet-}$ was attacked by h^+ to form the $^1O_2$. Finally, the sulfoxide product could be obtained from further oxidizing sulfide using the singlet oxygen. Another minor route is that the surface holes react with sulfide to form the corresponding intermediate which further reacts with $O_2^{\bullet-}$ to produce sulfoxide.

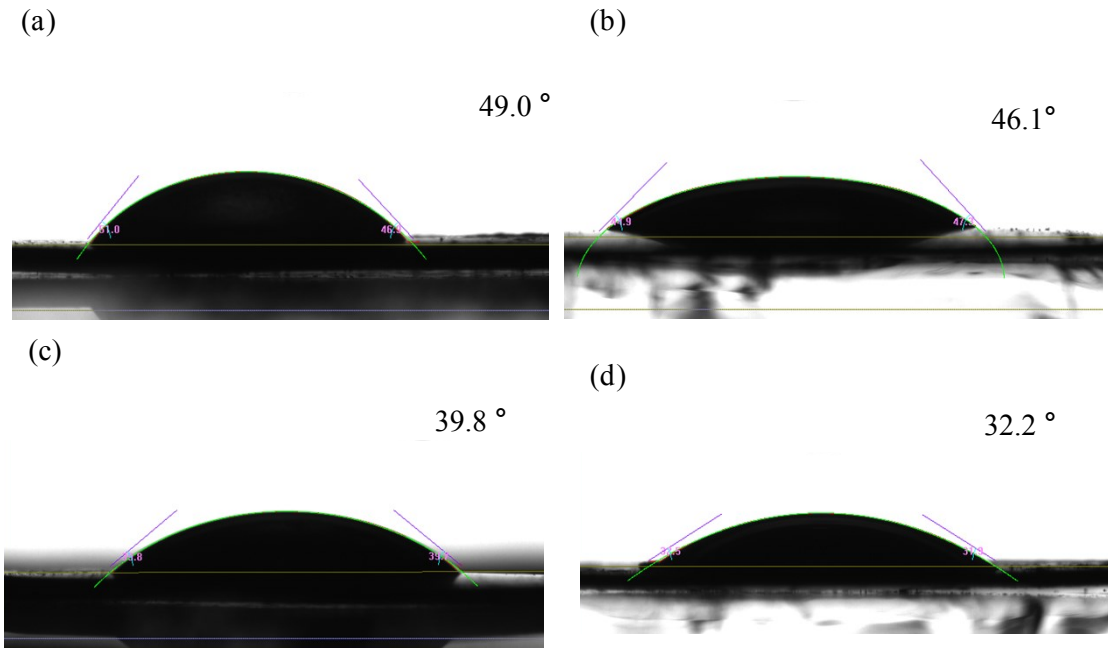

Fig. S19. Contact-angle of water on the surface of (a) C_3N_4, (b) COCN-3, (c) COCN-2 and (d) COCN-1.

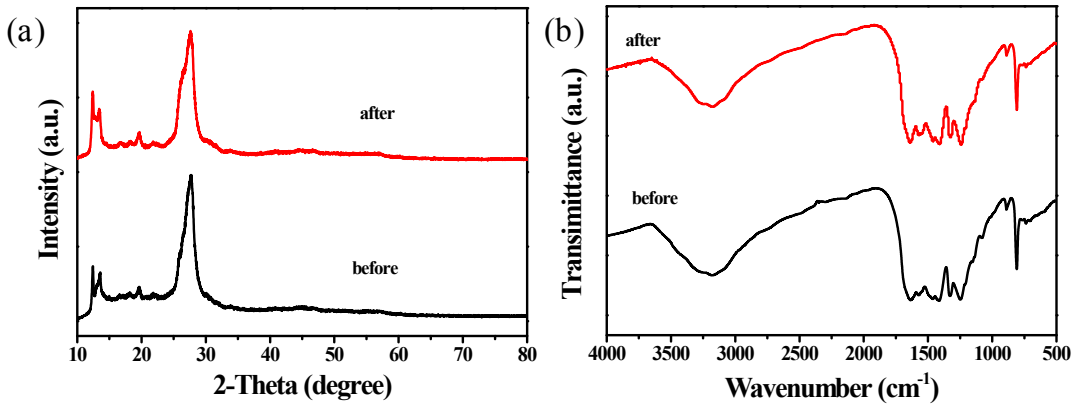

Fig. S20. (a) XRD and (b) FTIR spectra of COCN-2 before and after eight cycles for photocatalytic H_2 production.

REFERENCES

S1 J. Li, Y. Chen, X. Yang, S. Gao and R. Cao, *J. Catal.* 2020, **381**, 579.

S2 Y. Xu, Z.-C. Fu, S. Cao, Y. Chen and W.-F. Fu, *Catal. Sci. & Technol.* 2017, **7**, 587.

S3 X. Chen, K. Deng, P. Zhou and Z. Zhang, *ChemSusChem* 2018, **11**, 2444.

S4 X. Ma, H. Hao, W. Sheng, F. Huang and X. Lang, *J. Mater. Chem. A* 2021, **9**, 2214.

S5 X. Lan, Q. Li, Y. Zhang, Q. Li, L. Ricardez-Sandoval and G. Bai, *Appl. Catal. B: Environ.* 2020, **277**, 119274.

S6 J.-L. Shi and X. Lang, *Chem. Eng. J.* 2020, **392**, 123632.

S7 C. G. López-Calixto, S. Cabrera, R. Pérez-Ruiz, M. Barawi, J. Alemán, V. A. de la Peña O'Shea and M. Liras, *Appl. Catal. B: Environ.* 2019, **258**, 117933.

S8 L. Q. Wei and B. H. Ye, *ACS Appl. Mater. Inter.* 2019, **11**, 41448.

S9 X. N. Zou, D. Zhang, T. X. Luan, Q. Li, L. Li, P. Z. Li and Y. Zhao, *ACS Appl.*

Mater. Inter. 2021, https://doi.org/10.1021/acsami.1c03083

S10 X. Cheng, J. Zhang, L. Liu, L. Zheng, F. Zhang, R. Duan, Y. Sha, Z. Su and F. Xie, *Green Chem.* 2021, **23**, 1165.

S11 Y. Qian, D. Li, Y. Han and H.-L. Jiang, *J. Am. Chem. Soc.* 2020, **142**, 20763.

S12 A. López-Magano, A. E. Platero-Prats, S. Cabrera, R. Mas-Ballesté and J. Alemán, *Appl. Catal. B: Environ.* 2020, **272**, 119027.

S13 Q. Li, X. Lan, G. An, L. Ricardez-Sandoval, Z. Wang and G. Bai, *ACS Catal.* 2020, **10**, 6664.

S14 D.-Y. Zheng, E.-X. Chen, C.-R. Ye and X.-C. Huang, *J. Mater. Chem. A* 2019, **7**, 22084

S15 H. Wang, S. Jiang, S. Chen, D. Li, X. Zhang, W. Shao, X. Sun, J. Xie, Z. Zhao, Q. Zhang, Y. Tian and Y. Xie, *Adv. Mater.* 2016, **28**, 6940.

S16 Y. A. Workie, Sabrina, T. Imae, M. P. Krafft, *ACS Biomater. Sci. Eng.*, 2019, **5**, 2926.

S17 G. Zhang, Y. Xu, C. He, P. Zhang, H. Mi, *Appl. Catal. B: Environ.*, 2021, **283**, 119636.

S18 Y. Li, J. Ren, S. Ouyang, W. Hou, T. Petit, H. Song, H. Chen, D. Philo, T. Kako, J. Ye, *Appl. Catal. B: Environ.*, 2019, **259**, 118027.

S19 Y. Yu, W. Yan, X. Wang, P. Li, W. Gao, H. Zou, S. Wu, K. Ding, *Adv. Mater.* 2018, **30**, 1705060.

S20 Y. Ejeta, T. Imae, *J. Photoch. Photobio. A: Chem.*, 2021, **404**, 112955.

S21 H. Wang, X. Yang, W. Shao, S. Chen, J. Xie, X. Zhang, J. Wang, Y. Xie, *J. Am.*

Chem. Soc., 2015, **137**, 11376.

S22 S. Zhao, X. Zhao, *Appl. Catal. B: Environ*., 2019, **250**, 408.

S23 J. Jiang, R. Luo, X. Zhou, Y. Chen, H. Ji, *Adv. Synth. & Catal.*, 2018, **360**, 4402.

S24 X. Chen, K. Deng, P. Zhou, Z. Zhang, *ChemSusChem*, 2018, **11**, 2444.